The Astrophysical Journal Letters, 828:L20 (6pp), 2016 September 10 doi:10.3847/2041-8205/828/2/L20

THE FIRST DISTANCE CONSTRAINT ON THE RENEGADE HIGH-VELOCITY CLOUD COMPLEX WD

J. E. G. Peek[1], Rongmon Bordoloi[2], Hugues Sana[3], Julia Roman-Duval[1], Jason Tumlinson[1], and Yong Zheng[4]
[1] Space Telescope Science Institute, 3700 San Martin Drive, Baltimore, MD 21218, USA
[2] MIT-Kavli Center for Astrophysics and Space Research, 77 Massachusetts Avenue, Cambridge, MA 02139, USA
[3] Institute of Astronomy, KU Leuven, Celestijnenlaan 200 D, B-3001 Leuven, Belgium
[4] Department of Astronomy, Columbia University, New York, NY 10027, USA
Received 2016 July 19; revised 2016 August 16; accepted 2016 August 22; published 2016 September 9

ABSTRACT

We present medium-resolution, near-ultraviolet Very Large Telescope/FLAMES observations of the star USNO-A0600-15865535. We adapt a standard method of stellar typing to our measurement of the shape of the Balmer ϵ absorption line to demonstrate that USNO-A0600-15865535 is a blue horizontal branch star, residing in the lower stellar halo at a distance of 4.4 kpc from the Sun. We measure the *H* & *K* lines of singly ionized calcium and find two isolated velocity components, one originating in the disk, and one associated with the high-velocity cloud complex WD. This detection demonstrated that complex WD is closer than ∼4.4 kpc and is the first distance constraint on the $+100\,\mathrm{km\,s^{-1}}$ Galactic complex of clouds. We find that complex WD is not in corotation with the Galactic disk, which has been assumed for decades. We examine a number of scenarios and find that the most likely scenario is that complex WD was ejected from the solar neighborhood and is only a few kiloparsecs from the Sun.

Key words: Galaxy: evolution – Galaxy: formation – Galaxy: halo – ISM: atoms – ISM: clouds – ISM: kinematics and dynamics

1. INTRODUCTION

High-velocity clouds (HVCs) provide a unique window into the coolest component of the circumgalactic medium and the processes of Galactic inflow and outflow. HVCs, and the complexes into which they are arranged, are found by their emission in H I or absorption in numerous metal lines, and have radial velocities inconsistent with Galactic rotation (Wakker & van Woerden 1997). The precise origin of most HVCs is unknown, and some mix of Galactic fountain (e.g., Bregman 1980), multiphase accretion (e.g., Fernández et al. 2012), and gas stripping from satellites is typically invoked (Putman et al. 2012). The exception is the Magellanic stream, which was stripped from the large and small Magellenic clouds, and which we will exclude from our discussion in this work. HVCs with negative radial velocities, which have metalicities in the range of 10% to 30% of the solar metallicity, are likely a tracer of the process by which material accretes onto the Galaxy, though the total rate of this accretion is very uncertain. Less explored are the HVCs with positive radial velocities, most of which are in the inner two quadrants of the Galactic sky. These include the Wannier complexes WA, WB, WD, and WE, and the Smith Cloud (Wakker & van Woerden 1991). The Smith cloud has received significant attention of late because of its strongly cometary appearance, which provides enough information to infer past trajectories and to make some inference as to its origin (Lockman et al. 2008; Fox et al. 2015).

Complex WD is the largest-area positive velocity HVC complex, covering 310 square degrees, with a total H I flux of $1.2 \times 10^7\,\mathrm{K\,km\,s^{-1}\,arcmin^2}$, and a maximum H I column density of $\sim 1.2 \times 10^{20}\,\mathrm{cm^{-2}}$. It is by far the largest complex that exists in the inner two Galactic quadrants, where a small fraction of HVC flux is detected. With a range of velocities between +90 and $+130\,\mathrm{km\,s^{-1}}$ Local Standard of Rest (LSR; our convention for the remainder of this work), it is consistent with cylindrical rotation on the far side of the inner Galaxy, 20 kpc from the Sun, with a mass of $6 \times 10^7\,M_\odot$. This would make it very similar in mass, Galactocentric radius, and height to complex C, the largest-area and brightest HVC complex (Thom et al. 2008).

One major issue in gaining a better physical understanding of these enigmatic clouds is their unknown distance. Since there are no objects of fixed luminosity in HVCs, there are effectively no intrinsic distance measures. H I emission or optical and UV absorption lines toward extragalactic background sources only provide distance-independent column densities. HVC distances not only give us masses for these structures, but also a context; the spatial relationship between the cloud and the nearby spatial and kinematic structure of the disk gives us insight as to its origin.

There are a number of indirect methods for measuring the distance to an HVC complex, including Hα emission and kinematic structure (Putman et al. 2003; Peek et al. 2007), but the only proven direct distance measure is stellar absorption. By observing stars with measured distances at medium or high spectral resolution, one can look for absorption lines in Na I, Ca II H & K, Ti II, and numerous ultraviolet absorption lines at the velocity of H I emission from HVCs Schwarz et al. (1995). By finding detections and non-detections of these absorption lines along lines of sight toward H I-emitting HVCs, distances can be robustly measured. A number of clouds have well-measured distances using this method, but complex WD is not among them (Wakker 2001; Wakker et al. 2007, 2008; Thom et al. 2008; Lehner et al. 2012).

In this work we report the first distance upper limit on complex WD using medium-resolution absorption line spectroscopy toward a blue horizontal branch (BHB) star. We extend the methods of Sirko et al. (2004) to find the spectral type of the star, and thus find a precise distance limit. We use this to make some inferences as to the possible origin of complex WD, and how it fits into the structure of Galactic HVCs as a whole.

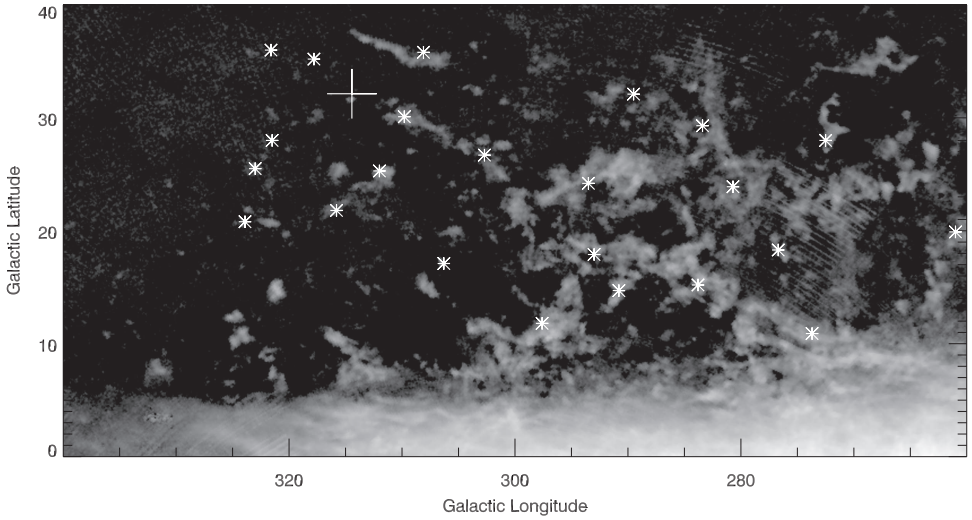

Figure 1. Complex WD. The grayscale is the H I-integrated column density between 98 and 131 km s^{-1} on a log scale in Galactic coordinates. The feature below 5° is the Galactic plane, while the rest of the structure is complex WD, stretching from 260° to 325° in Galactic latitude and 5° to 40° in Galactic latitude. The asterisks are the locations of the WD clouds in the Wakker van Woerden 1991 catalog. The cross is the location of USNO-A0600-15865535 (l = 314.43854, b = 32.13507). The faint, parallel arc-like structures are systematic errors in the GASS data reduction.

2. DATA

2.1. New Observations

The observations of our target, USNO-A0600-15865535, were obtained at the ESO Very Large Telescope (VLT) at Cerro Paranal, Chile on the nights of 2016 May 6th and May 7th. The target was observed as a part of our program "Mapping the Cool Circumgalactic Medium with Calcium II" (097.A-0552, PI: Peek), which uses the FLAMES/GIRAFFE spectrograph, a fiber-fed multiobject spectrograph mounted on the Nasmyth focus of UT2 (Pasquini et al. 2003). USNO-A0600-15865535 is a bright ($g = 14.2$) very blue ($g - r = -0.21$) source, unresolved in Pan-STARRS imaging (Schlafly et al. 2012; Tonry et al. 2012; Magnier et al. 2013). Through a combination of over-optimism and clerical error, it was targeted as a quasar candidate behind the circumgalactic medium of M83.

The GIRAFFE High Resolution mode was used in the H395.8 setup (HR02), which enables access to the 385.4 to 404.9 nm wavelength range in the near-UV at a spectral resolving power $\lambda/\delta\lambda$ of 22,700. A total of 4.5 hr of integration were obtained, split in 3 exposures of 90 minutes. Given that most of the program targets were faint, the non-standard 50 khz, 1 × 1, high gain readout mode was used (Melo et al. 2008). Corresponding calibration frames were obtained within 24 hr of the science observations. The raw scientific data were bias- and dark-subtracted, flat-fielded, and wavelength-calibrated using the instrument's pipeline v12.14.2 under the esorex environment. The source spectra were extracted in the SUM mode. Finally the individual exposures were summed up to improve the signal-to-noise ratio (S/N) of the extracted data.

2.2. Archival Data

In addition to the new data taken with FLAMES, we also used archival H I data from the GASS survey (Kalberla et al. 2010). GASS is a survey of Galactic H I taken with the Parkes antenna, with a beam size of 16′, a spectral resolution of 1 km s^{-1}, and an rms noise of 57 mK. These data allow us to map out the structure of complex WD on the sky, and compare the spectrum of the H I emission to Ca II H & K absorption along the line of sight. In Figure 1 we present an image of complex WD from GASS, along with the positions of clouds found in the Wakker & van Woerden (1991) catalog, and the line of sight toward USNO-A0600-15865535.

3. METHODS AND RESULTS

3.1. Stellar Classification

The $R = 22700$, high S/N spectra of USNO-A0600-15865535 showed it to have very strong Hϵ and Hζ at ∼0 km s^{-1} in the LSR frame, and thus making it very likely to be a halo star in the Milky Way, rather than the quasar that we had originally attempted to target. Such stars are typically either BHB stars or blue stragglers (BS) stars, though they can occasionally be hot main sequence (MS) stars.

To distinguish between these possibilities, we use a modification of the method developed by Sirko et al. (2004) and later explored by Xue et al. (2008). In these works the shapes of the Hγ and Hδ lines are used to distinguish between these populations. These Balmer lines are fit with a standard Sersić profile,

$$y = 1 - a \exp\left[-\left(\frac{|\lambda - \lambda_0|}{b}\right)^c\right] \quad (1)$$

and the parameters measured for these lines are distinct between the populations. Unfortunately, we do not have observations of the Hγ or Hδ line, only the Hϵ and Hζ lines. To determine whether we can use the (better resolved) Hϵ line as a similar discriminator, we first assemble a sub-population of BHB, BS, and MS drawn from the catalog presented in Xue et al. (2008), selected to be brighter than the 16th magnitude in g. These targets have already been fit and classified, but to test our method we refit the Hγ line in the SDSS DR10 spectra using Equation (1). We find that we can indeed reproduce the bifurcation between BHB and BS stars. We then apply this

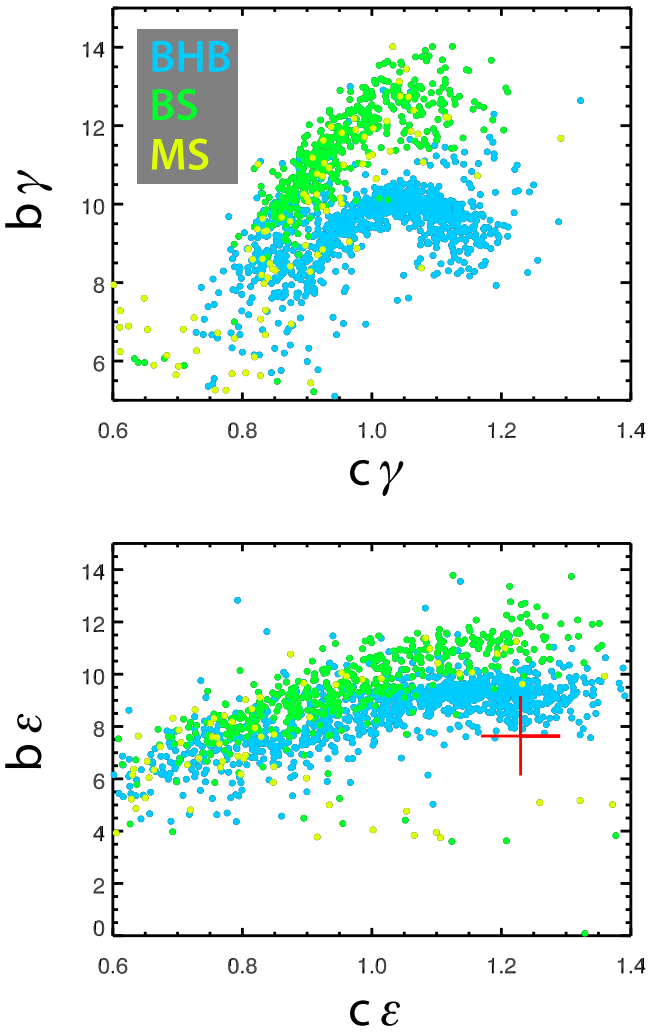

Figure 2. Sersić parameters of the Hγ (top) and Hϵ (bottom) lines as measured in 1637 stars from Xue et al. (2008) with $g < 16$. Overplotted in the bottom panel in a red cross is the result for the FLAMES spectrum of USNO-A0600-15865535, clearly a BHB star.

same fitting procedure to the Hϵ line. The results for both fits are shown in Figure 2. The Hϵ line fit Sersić parameters b and c do not as clearly delineate between BHB and BS stars, but the differentiation is still very much in place. We then apply this same fit to our VLT/FLAMES spectrum of USNO-A0600-15865535, and overplot the b and c parameters. USNO-A0600-15865535 is clearly a BHB star.

BHB stars have the useful property of being accurate standard candles. There is a direct relationship between BHB color and absolute magnitude reported in Xue et al. (2008; these values are originally reported in Sirko et al. 2004 with a typographical error). The observed color in Pan-STARRS1 imaging is $g - r = -0.21$, and Schlegel et al. (1998) report a reddening of $E(B-V) = 0.068$ toward this sightline, giving us a corrected color of $g - r = -0.28$ using the parameters from Schlafly & Finkbeiner (2011). Using the correspondence reported in Sirko et al. (2004), this translates to an absolute magnitude of $M_g = 0.8$. USNO-A0600-15865535's measured g magnitude of 14.2, reddening-corrected to 14.0, gives a final distance of 4.4 kpc, with distance errors for BHB stars typically quoted at 10%.

Table 1
Voigt Profile Fit Parameters for the Calcium II H & K Lines

b [km s^{-1}]	$v_{\rm LSR}$ [km s^{-1}]	log(N [cm^{-2}])
6.3 ± 1.8	−6.6 ± 0.6	12.05 ± 0.08
20.7 ± 1.7	0.7 ± 1.7	12.15 ± 0.07
11.8 ± 22.2	92.3 ± 36.7	11.58 ± 0.80
10.4 ± 4.1	108.1 ± 7.1	12.17 ± 0.46

3.2. ISM Line Measurement

We perform a Voigt-profile-fitting of the calcium II H & K lines after dividing out the continuum spectrum, and in the case of the calcium II H lines, dividing out the Sersić fit to the strong Hϵ line, which is centered at 230 km s^{-1} LSR in the calcium II H frame. The column densities were determined by simultaneously fitting Voigt profiles to both lines of the Ca II doublet with the VPFIT software.[1] For our Voigt profile fit analysis, the intrinsic model profiles are convolved with a Gaussian of FWHM 14 km s^{-1} to account for the instrument resolution. The Ca II line close to the Milky Way rest frame is best fit with two Voigt profile components centered at $v_{\rm LSR} \approx -6$ and 1 km s^{-1}. The redshifted high-velocity absorption component is best fit with two Voigt profile components centered at $v_{\rm LSR} \approx 92.3$ and 108 km s^{-1}. All four individual Voigt profile components to Ca II K components agree with the equivalent Ca II H parameters to within the errors. The individual Voigt profile fits are reported in Table 1 and are shown in Figure 3.

Three main H I components are detected—one near $v_{\rm LSR} = 0$, one corresponding to the HVC at $v_{\rm LSR} = 100$ and an intermediate velocity component. The H I column densities for each of these components are found by integrating the flux under the line under the optically thin assumption. We find a column density of 4.6×10^{20} cm^{-2}, 2.2×10^{19} cm^{-2}, and 8.6×10^{18} cm^{-2} for the low, intermediate, and high-velocity components, respectively.

4. DISCUSSION

The clear detection of Ca II H & K absorption at +100 km s^{-1} in USNO-A0600-15865535, coincident with H I emission from complex WD, indicates that the complex is closer than the star, at a distance of 4.4 kpc. If the whole complex were 4.4 kpc from the Sun, it would have an H I mass of $2.8 \times 10^5\ M_\odot$. The column of Ca II measured is comparable between the cloud and the disk, even though they have wildly different H I columns. This is consistent with the weak (Wakker & Mathis 2000) or non-existent (Ben Bekhti et al. 2012) correlation between H I and Ca II column density, which also explains the non-detection of the small intermediate velocity cloud along the line of sight at 60 km s^{-1}. Unfortunately, this lack of correlation makes it impossible to infer anything about the metallicity of the cloud from these metal absorption lines. Future metallicity measurements, perhaps toward USNO-A0600-15865535, will be critical for determining the origin of complex WD, as gas of extragalactic origin is expected to have lower metallicities.

The kinematics and location of complex WD do give us some clues as to its origin. Originally, Wakker & van Woerden (1991) suggested that because complex WD is at a positive velocity, it is likely part of the structure of the Galaxy itself,

[1] Available at http://www.ast.cam.ac.uk/~rfc/vpfit.html

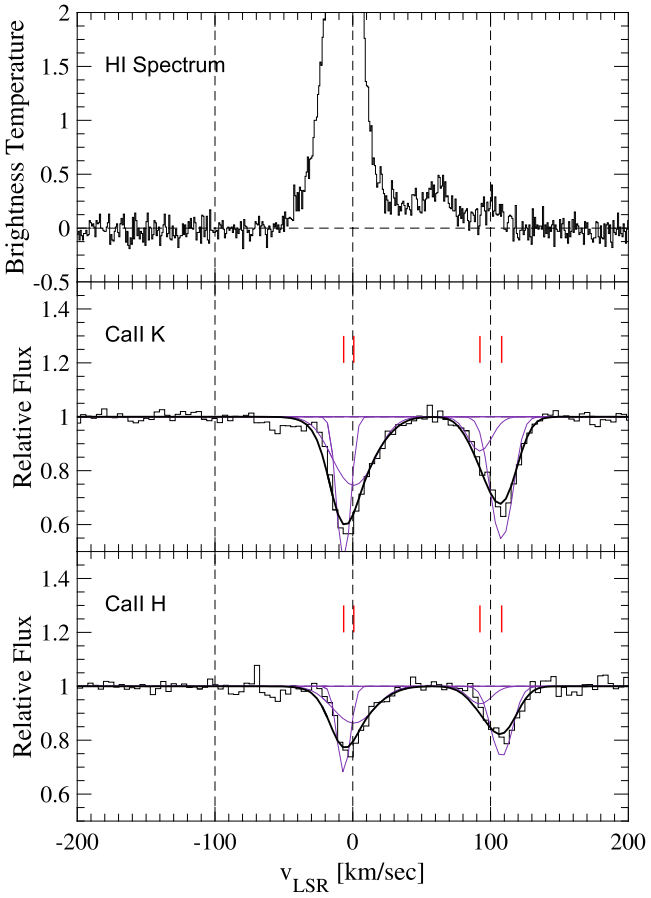

Figure 3. H I and Ca II toward USNO-A0600-15865535. The top panel is the GASS spectrum toward USNO-A0600-15865535, stretched to show the faint HVC feature at 100 km s^{-1}. The two bottom panels are the Ca II K and H absorption line features, clearly showing the HVC absorption. The vertical red ticks show the location of the centroids of individual Voigt profile fits.

corotating with the disk. We call this the "far" scenario in Figure 4, and it is emphatically ruled out by our detection of absorption. The appeal of the scenario is quite clear from the figure—a cloud at 20 kpc could be corotating with the disk. We now know that complex WD is mostly inside the solar circle toward the fourth quadrant. Along the line of sight to USNO-A0600-15865535, complex WD sits above a portion of the disk moving at -30 km s^{-1} LSR if we assume that it is at the maximal distance of 4.4 kpc (H I mass of 2.8×10^5 $M_\odot$), decreasing to 0 km s^{-1} LSR as we assume a closer distance. Complex WD is therefore strongly not in corotation with the disk. This is in rather stark contrast with other HVCs; a simplified model of HVCs with known distances found that they rotated with the disk at 77 km s^{-1}—slower than Galactic rotation, but with the same logic (Putman et al. 2012).

A number of scenarios could account for the overall difference in velocity between the cloud and the disk. An accreting cloud could easily have a much lower accretion velocity than the rotation speed of the disk, and the positive velocity observed could be an artifact of the solar motion. Similarly, it is possible that complex WD is material ejected from star-forming regions closer to the Galactic center (e.g., Ford et al. 2010), and thus the high positive velocity is an effect of the lower specific angular momentum of that material. Both of these scenarios suffer from the fine-tuning required to meet the very small LSR velocity gradient found in the complex. A flux-weighted first-order polynomial fit to the velocity gradient in the Wakker & van Woerden (1991) catalog of WD clouds finds -0.072 ± 0.146 km s^{-1} per degree of Galactic longitude. The reflex velocity of the solar motion represents 100 km s^{-1} across 40° of complex WD—unless the cloud is conspiring to thwart our detection of a velocity gradient, we should see some effect of the solar motion. While we cannot fully rule out the "intermediate" scenario, where the bulk of the cloud is at ~4 kpc, this velocity structure puts very tight constraints on any future model.

Finally we examine a "near" scenario, where complex WD is only 1–2 kpc away. At 1.5 kpc, the cloud has an H I mass of only 3.3×10^4 $M_\odot$. In this scenario the cloud originated from an area near the Sun, and thus has inherited the overall solar motion. Since all the gas started with the 3-space velocity of the solar neighborhood, there is no need for fine-tuning of the LSR velocity. In the "near" scenario the cloud is ejected from the disk by some kind of impulsive event, perhaps connected to star formation in the Gould Belt or Saggitarus Arm, imparting an overall 100 km s^{-1} bulk velocity radially away from the solar vicinity. This corresponds to kinetic energy of 6.6×10^{51} erg, equivalent to the energy of a handful of supernovae. If the energy is imparted from precisely the position of the Sun, then the explosive motion of the gas will be exactly measured as radial velocity, consistent with the observation of an undetectable velocity gradient. We can ask if this model creates a different fine-tuning problem: how far can this explosive event be from the Sun before we see too large a gradient in the LSR velocity field? As an example, if the event originated in an area toward the center of complex WD from the Sun by some distance R_e, the center of the WD would have the explosive velocity V_e, while the edge, about 30° away, would have a velocity $V_e \sin(\alpha)$, where α is the angle formed by the lines that connect the edge of the cloud to both the event origin and to the Sun. If we allow a gradient of no more than 0.146 km s^{-1} per degree of Galactic longitude, and complex WD is assumed to be 2 kpc away, from the law of sines we find $R_e < 270$ pc. This exercise can be repeated for all displacements from the Sun, and we find similar results—the explosive event must have originated from within 270 pc of the Sun. This defines a rather large area of the disk with a number of currently active star-forming regions, and thus we do not consider this to be too tight of a constraint. We note that a cloud that is 2 kpc toward complex WD would only be about 0.5 kpc above the disk, which is quite low for most known HVCs, and would make it distinct from all other known HVCs in its origin, although farther away low-altitude HVCs might well blend into gas along the line of sight. The shearing effect of differential rotation is much weaker close to the Sun, which makes this impulsive scenario more credible for a closer cloud. The somewhat symmetric complex WE, with a similar velocity and location but at a negative Galactic latitude, could conceivably have been generated by the same event.

5. CONCLUSIONS

In this work we have found that while the Hϵ line is not as powerful a discriminant between BHB, BS, and MS stars as the Hγ or Hδ line, it can be used to show that USNO-A0600-15865535 is a BHB star that is approximately 4.4 kpc from the Sun. We have demonstrated that this star has clear Calcium *H* & *K* absorption lines at a velocity coincident with complex WD, and that therefore complex WD must be closer than

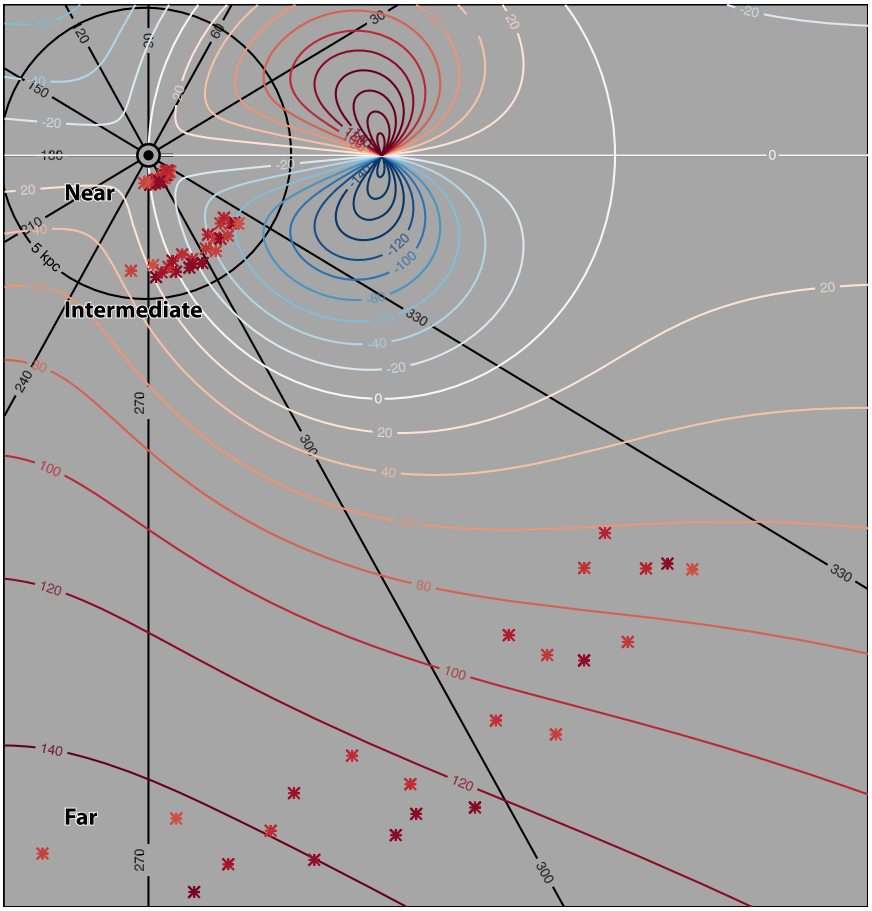

Figure 4. A top-down view of the Galaxy. Lines of constant Galactic longitude are shown in black, meeting at the Sun, marked by ⊙. The colored lines represent the LSR velocity of the gas in the Galactic disk expected from a flat, 220 km s^{-1} rotation curve, with bluer contours representing more negative velocities, and redder contours representing more positive velocities. The asterisks are the complex WD clouds found in Wakker & van Woerden (1991), colored according to their LSR velocities with the same scheme as that for the disk. We show three distance scenarios: the original "far" scenario, which this work has ruled out, an "intermediate" scenario, where all clouds are put at 4.4 kpc, and a "near" scenario, where all clouds are 1 kpc from the Sun.

4.4 kpc. We used this fact to rule out the originally assumed model of complex WD, that is, a complex C-like cloud on the far side of the Galaxy, corotating with disk. Furthermore, we investigated an intermediate distance scenario in which the complex resides at ∼4 kpc and found it difficult to reconcile the fixed LSR velocity of the cloud with the strong gradients implied from both the reflex solar motion and differential Galactic rotation. A "near" scenario, wherein the complex was ejected from the solar vicinity to a distance of a few kiloparsecs, seemed the most likely, though it would make the HVC the lowest known HVC in altitude, making complex WD somewhat of a renegade in the HVC family.

Future observations toward USNO-A0600-15865535 would enable precise determinations of metallicities using other elements, which would help determine whether a disk-origin for this cloud is likely. Further observations toward closer stars, and across the face of the cloud could, give us much more detailed information about the distance and three-dimensional morphology of the cloud, which would also help us understand how the cloud came to be, and how it relates to the accretion and feedback story of the Milky Way.

The authors thank Jessica Werk and Alis Deason for advice on the BHB spectroscopic determination method. This work is based on observations made with ESO Telescopes at the La Silla Paranal Observatory under program ID 097.A-0552. This work used Pan-STARRS1 data for targeting USNO-A0600-15865535 and accurate *g* and *r* band photometry. The Pan-STARRS1 Surveys have been made possible through contributions of the Institute for Astronomy, the University of Hawaii, the Pan-STARRS Project Office, the Max Planck Society and its participating institutes, the Max Planck Institute for Astronomy, Heidelberg and the Max Planck Institute for Extraterrestrial Physics, Garching, The Johns Hopkins University, Durham University, the University of Edinburgh, Queen's University Belfast, the Harvard-Smithsonian Center for Astrophysics, the Las Cumbres Observatory Global Telescope Network Incorporated, the National Central University of Taiwan, the Space Telescope Science Institute, the National Aeronautics and Space Administration under grant No. NNX08AR22G issued through the Planetary Science Division of the NASA Science Mission Directorate, the National Science Foundation under grant No. AST-1238877, the University of Maryland, and Eotvos Lorand University (ELTE), and the Los Alamos National Laboratory.

REFERENCES

Ben Bekhti, N., Richter, P., Winkel, B., et al. 2012, in EAS Publ. Ser. 56, The Role of Disk-Halo Interaction in Galaxy Evolution: Outflow vs. Infall?, ed. M. A. de Avillez (Les Ulis: EDP Sciences), 513

Bregman, J. N. 1980, ApJ, 236, 577
Fernández, X., Joung, M. R., & Putman, M. E. 2012, ApJ, 749, 181
Ford, H. A., Lockman, F. J., & McClure-Griffiths, N. M. 2010, ApJ, 722, 367
Fox, A. J., Lehner, N., Lockman, F. J., et al. 2015, ApJL, 816, L11
Kalberla, P. M. W., McClure-Griffiths, N. M., Pisano, D. J., et al. 2010, A&A, 521, A17
Lehner, N., Howk, J. C., Thom, C., et al. 2012, MNRAS, 424, 2896
Lockman, F. J., Benjamin, R. A., Heroux, A. J., & Langston, G. I. 2008, ApJL, 679, L21
Magnier, E. A., Schlafly, E., Finkbeiner, D., et al. 2013, ApJS, 205, 20
Melo, C., Pasquini, L., Downing, M., et al. 2008, Msngr, 133, 17
Pasquini, L., Alonso, J., Avila, G., et al. 2003, Proc. SPIE, 4841, 1682
Peek, J. E. G., Putman, M. E., McKee, C. F., Heiles, C., & Stanimirović, S. 2007, ApJ, 656, 907
Putman, M., Peek, J., & Joung, M. 2012, ARA&A, 50, 491
Putman, M. E., Bland-Hawthorn, J., Veilleux, S., et al. 2003, ApJ, 597, 948
Schlafly, E. F., & Finkbeiner, D. P. 2011, ApJ, 737, 103
Schlafly, E. F., Finkbeiner, D. P., Jurić, M., et al. 2012, ApJ, 756, 158
Schlegel, D. J., Finkbeiner, D. P., & Davis, M. 1998, ApJ, 500, 525
Schwarz, U. J., Wakker, B. P., & van Woerden, H. 1995, A&A, 302, 364
Sirko, E., Goodman, J., Knapp, G. R., et al. 2004, AJ, 127, 899
Thom, C., Peek, J. E. G., Putman, M. E., et al. 2008, ApJ, 684, 364
Tonry, J. L., Stubbs, C. W., Lykke, K. R., et al. 2012, ApJ, 750, 99
Wakker, B. P. 2001, ApJS, 136, 463
Wakker, B. P., & Mathis, J. S. 2000, ApJL, 544, L107
Wakker, B. P., & van Woerden, H. 1991, A&A, 250, 509
Wakker, B. P., & van Woerden, H. 1997, ARA&A, 35, 217
Wakker, B. P., York, D. G., Howk, J. C., et al. 2007, ApJL, 670, L113
Wakker, B. P., York, D. G., Wilhelm, R., et al. 2008, ApJ, 672, 298
Xue, X. X., Rix, H. W., Zhao, G., et al. 2008, ApJ, 684, 1143